Scattering of electromagnetic waves from a bounded medium with a random surface

J. A. Sánchez-Gil and A. A. Maradudin
Department of Physics and Institute for Surface and Interface Science, University of California, Irvine, California 92717

Jun Q. Lu
Surface Optics Corporation, P.O. Box 261602, San Diego, California 92126

V. D. Freilikher, M. Pustilnik, and I. Yurkevich
The Jack and Pearl Resnick Institute of Advanced Technology, Department of Physics, Bar-Ilan University, Ramat-Gan 52900, Israel
(Received 10 May 1994)

By small-amplitude perturbation theory and by a computer-simulation approach we have studied the incoherent scattering of electromagnetic waves from a randomly rough, dielectric film deposited on a planar, perfectly conducting surface. The thickness of the dielectric film is such that in the absence of the roughness the scattering system supports two guided waves. As a consequence, each multiply scattered wave is now degenerate. The coherent interference of each of these degenerate waves with the waves obtained from them by time reversal produces two satellite peaks in the angular dependence of the intensity of the incoherent component of the scattered field, in addition to the enhanced backscattering peak. These satellite peaks occur at scattering angles θ_s that are related to the angle of incidence θ_0 by $\sin\theta_s = -\sin\theta_0 \pm (c/\omega)[q_1(\omega) - q_2(\omega)]$, where $q_1(\omega)$ and $q_2(\omega)$ are the wave numbers of the two guided waves supported by the scattering system at the frequency ω of the incident field. These peaks are present in the results of both the perturbation and simulation calculations. They are shown to be multiple-scattering effects, and not a single-scattering phenomenon.

I. INTRODUCTION

A great deal of attention has been paid recently to the multiple scattering of classical waves and quantum particles from systems with volume and surface disorder. The interest in this problem was stimulated by the fact that in disordered media, notwithstanding the seemingly absolutely random nature of the scatterers (either volume or surface), under certain conditions there occurs either complete [one-dimensional (1D) systems] or partial (2D and 3D systems) coherence of the multiply scattered fields. This coherence, which is a consequence of time-reversal symmetry, leads to a constructive interference that gives rise to such effects as strong localization,[1] fluctuational waveguiding,[2] weak localization,[3] enhanced backscattering,[4] the memory effect,[5] etc. Until recently, in the investigation of these phenomena attention was directed mainly on infinite systems. However, in bounded random media, together with the random interaction of the fields it is often the case that regular interference, caused by the presence of surfaces, can also be significant. The additional coherence arising from the latter source leads to new effects absent in infinite systems.

In this paper we show analytically and numerically that the angular dependence of the intensity of waves scattered from a random bounded system with a discrete spectrum of excitations (a thin, randomly rough dielectric film deposited on a perfectly conducting substrate) exhibits, due to degenerate time-reversal symmetry, satellite peaks in addition to the enhanced backscattering peak that is characteristic for scattering from a random, semi-infinite medium.

To understand the physical origin of the enhancement of scattering into directions other than the retroreflection direction, we recall how the enhanced backscattering peak arises in the scattering from semi-infinite random media. In this case to each multiple-scattering path *ABCD* [Fig. 1(a)] that contributes to the field scattered into the retroreflection direction, there always corresponds a time-reversed partner *DCBA* that has exactly the same phase factor. As a result, these two waves are always coherent, notwithstanding the random positions of the scatterers. Note that in order that there be this coherence (equality of phases) the speeds of propagation from *C* to *B* and *B* to *C* must be equal.

In the case of a bounded system, the situation is more complicated. If the index of refraction $n_d = \sqrt{\epsilon_d}$ of the film is larger than those of the media bounding it, the

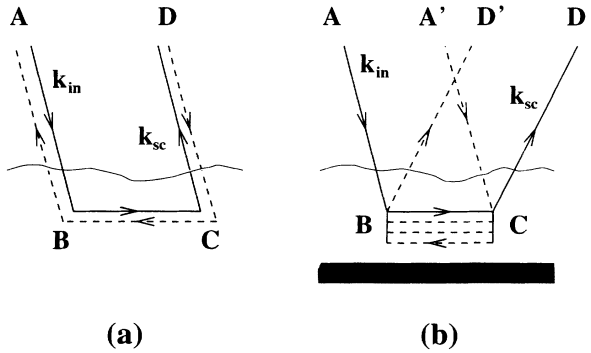

FIG. 1. Optical paths with the same phase factors. (a) An infinite medium, (b) a bounded medium.

0163-1829/94/50(20)/15353(16)/$06.00

transverse component of the wave vector $\mathbf{k}$ is quantized inside the film. The field corresponding to the discrete part of the spectrum is the sum of guided eigenwaves, each of which propagates along the film with its own (quantized) phase velocity. In contrast to the situation in an infinite or semi-infinite medium, each trajectory *ABCD* [Fig. 1(b)] is now N fold degenerate, where N is the number of discrete modes supported by the waveguide, in the sense that along the segment *BC* there are N "channels" with different phase factors. The phase difference for the two paths $(ABCD)_n$ and $(A'CBD')_m$ is equal to[6]

$$\Delta\phi_{nm}=(\mathbf{k}_{\rm in}+\mathbf{k}_{\rm sc})\cdot\mathbf{r}_{BC}+(k_n-k_m)|\mathbf{r}_{BC}|\ , \tag{1.1}$$

where $\mathbf{k}_{\rm in}$ and $\mathbf{k}_{\rm sc}$ are the wave vectors of the incident and scattered waves, respectively, the vector $\mathbf{r}_{BC}$ connects the scatterers B and C, and k_i is the wave number of the ith mode. We see from Eq. (1.1) that constructive interference ($\Delta\phi_{nm}=0$) can occur not only for scattering into the retroreflection direction ($n=m$, $\mathbf{k}_{\rm sc}=-\mathbf{k}_{\rm in}$), which is the case for infinite and semi-infinite media, where $k_n=k_m=k$, but also for scattering into other directions $\mathbf{k}_{\rm sc}\neq-\mathbf{k}_{\rm in}$ for which $\Delta\phi_{nm}=0$ for some $n\neq m$.

The outline of the paper is as follows. In Sec. II we define the system studied in this work, viz., a thin dielectric film deposited on a perfectly conducting substrate, with a one-dimensional, randomly rough dielectric-vacuum interface, and a planar dielectric-conductor interface. The s-polarized guided waves supported by this structure in the absence of the roughness play a central role in the theory developed here.

Consequently, in Sec. III we derive the dispersion relation for these guided modes, and discuss those of their properties that will be needed in the remainder of this paper. In Sec. IV, the incoherent scattering of an s-polarized plane wave, whose plane of incidence is perpendicular to the generators of the random dielectric-vacuum interface, is calculated on the basis of a perturbative calculation of the scattering amplitude to third order in the surface-profile function. This low-order approximation is sufficient to reveal the peaks in the angular dependence of the intensity of the field that has been scattered incoherently, caused by the interference between inequivalent time-reversed scattering sequences arising from the existence of two or more degenerate guided-wave polaritons in the scattering structure. These perturbative calculations inform the computer-simulation studies of the scattering of a finite beam of s-polarized waves from the same structure carried out in Sec. V, whose results also display the additional peaks found perturbatively. A discussion of the results obtained, and the conclusions drawn from them, is presented in Sec. VI. An Appendix, in which the perturbative results obtained in Sec. IV are related to the many-body perturbation theory approach of Freilikher, Pustilnik, and Yurkevich[6] to this problem, concludes this paper.

II. THE SYSTEM STUDIED

In this paper we study the scattering of s-polarized light, whose plane of incidence is the x_1x_3 plane, that is

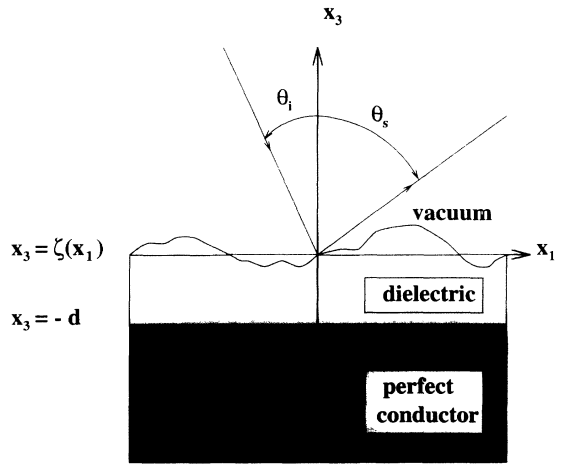

FIG. 2. The scattering system studied in this work.

incident from the vacuum side on a system that consists of vacuum in the region $x_3>\zeta(x_1)$, a dielectric film characterized by a dielectric constant ϵ_d in the region $-d<x_3<\zeta(x_1)$, and a perfect conductor in the region $x_3<-d$ (Fig. 2). The surface-profile function $\zeta(x_1)$ is assumed to be a continuous, single-valued function of x_1, that is differentiable as many times as is necessary. In addition, we assume that $\zeta(x_1)$ is a stationary, Gaussian, random process defined by the properties

$$\langle\zeta(x_1)\rangle=0\ , \tag{2.1}$$

$$\langle\zeta(x_1)\zeta(x_1')\rangle=\delta^2W(|x_1-x_1'|)\ . \tag{2.2}$$

In Eqs. (2.1) and (2.2), the angle brackets denote an average over the ensemble of realizations of $\zeta(x_1)$, while $\delta=\langle\zeta^2(x_1)\rangle^{1/2}$ is the rms height of the surface. In numerical calculations, we will use the Gaussian form

$$W(|x_1|)=\exp(-x_1^2/a^2) \tag{2.3}$$

for the surface height correlation function. The characteristic length a appearing in this expression is called the transverse correlation length of the surface roughness.

It is convenient to introduce the Fourier integral representation of $\zeta(x_1)$,

$$\zeta(x_1)=\int_{-\infty}^{\infty}\frac{dk}{2\pi}\hat{\zeta}(k)\exp(ikx_1)\ . \tag{2.4}$$

The Fourier coefficient $\hat{\zeta}(k)$ is also a Gaussian random process that possesses the following statistical properties:

$$\langle\hat{\zeta}(k)\rangle=0\ , \tag{2.5}$$

$$\langle\hat{\zeta}(k)\hat{\zeta}(k')\rangle=2\pi\delta(k+k')\delta^2g(|k|)\ . \tag{2.6}$$

The power spectrum of the surface roughness $g(|k|)$ appearing in Eq. (2.6) is defined by

$$g(|k|)=\int_{-\infty}^{\infty}dx_1\,W(|x_1|)\exp(-ikx_1)\ . \tag{2.7}$$

The form of $g(|k|)$ that corresponds to the choice of $W(|x_1|)$ given by Eq. (2.3) is

$$g(|k|)=\pi^{1/2}a\exp(-k^2a^2/4)\ . \tag{2.8}$$

III. GUIDED WAVES

A central role in the scattering theory developed in this paper is played by the guided waves supported by the scattering system in the limit that $\zeta(x_1)\equiv 0$. In this section we obtain the dispersion relation for these modes and determine their properties that will be needed in what follows.

In an s-polarized electromagnetic field whose plane of incidence is the x_1x_3 plane, the electric vector has the form

$$\mathbf{E}(\mathbf{x};t)=[0,E_2(x_1,x_3|\omega),0]\exp(-i\omega t) . \tag{3.1}$$

The amplitude $E_2(x_1,x_3|\omega)$ is the solution of

$$\left[\frac{\partial^2}{\partial x_1^2}+\frac{\partial^2}{\partial x_3^2}+\frac{\omega^2}{c^2}\right]E_2^{>}(x_1,x_3|\omega)=0 \tag{3.2}$$

in the region $x_3>0$, and is the solution of

$$\left[\frac{\partial^2}{\partial x_1^2}+\frac{\partial^2}{\partial x_3^2}+\epsilon_d\frac{\omega^2}{c^2}\right]E_2^{<}(x_1,x_3|\omega)=0 \tag{3.3}$$

in the region $-d<x_3<0$. The boundary conditions that must be satisfied at the interface $x_3=0$ are that the tangential components of the electric and magnetic fields must be continuous across it. These conditions can be written in the forms

$$E_2^{>}(x_1,x_3|\omega)|_{x_3=0}=E_2^{<}(x_1,x_3|\omega)|_{x_3=0} , \tag{3.4a}$$

$$\frac{\partial}{\partial x_3}E_2^{>}(x_1,x_3|\omega)|_{x_3=0}=\frac{\partial}{\partial x_3}E_2^{<}(x_1,x_3|\omega)|_{x_3=0} . \tag{3.4b}$$

At the same time $E_2^{>}(x_1,x_3|\omega)$ must vanish at $x_3=\infty$ in a guided wave, while $E_2^{<}(x_1,x_3|\omega)$ must vanish on the perfectly conducting surface $x_3=-d$.

The solution of Eq. (3.2) that describes a wave propagating in the x_1 direction whose amplitude vanishes at $x_3=\infty$ can be written in the form

$$E_2^{>}(x_1,x_3|\omega)=Ae^{iqx_1-\beta_0(q,\omega)x_3} , \tag{3.5}$$

where $\beta_0(q,\omega)=[q^2-(\omega^2/c^2)]^{1/2}$. The solution of Eq. (3.3) that describes a wave propagating in the x_1 direction and has the nature of a standing wave across the film that vanishes at $x_3=-d$ is

$$E_2^{<}(x_1,x_3|\omega)=Be^{iqx_1}\sin\alpha_d(q,\omega)(x_3+d) , \tag{3.6}$$

where $\alpha_d(q,\omega)=[\epsilon_d(\omega^2/c^2)-q^2]^{1/2}$.

The boundary conditions (3.4) yield the pair of equations

$$A=B\sin\alpha_d(q,\omega)d , \tag{3.7a}$$

$$-\beta_0(q,\omega)A=\alpha_d(q,\omega)B\cos\alpha_d(q,\omega)d , \tag{3.7b}$$

for which the solvability condition is

$$\beta_0(q,\omega)=-\alpha_d(q,\omega)\cot\alpha_d(q,\omega)d . \tag{3.8}$$

Equation (3.8) is the dispersion relation for the s-polarized guided waves supported by a dielectric film on a perfectly conducting substrate. These guided waves exist only in the region of the (ω,q) plane defined by the inequalities

$$(\omega/c)<q<\sqrt{\epsilon_d}(\omega/c) . \tag{3.9}$$

To solve Eq. (3.8), we define the variables x and y by

$$x=\alpha_d(q,\omega)d , \quad y=\beta_0(q,\omega)d . \tag{3.10}$$

Then, Eq. (3.8) becomes

$$y=-x\cot x . \tag{3.11}$$

A second relation between x and y is obtained if we first rewrite Eq. (3.10) in the forms

$$q^2=\epsilon_d\frac{\omega^2}{c^2}-\frac{x^2}{d^2} , \quad q^2=\frac{\omega^2}{c^2}+\frac{y^2}{d^2} . \tag{3.12}$$

When we eliminate q from this pair of equations, we obtain

$$y=(R^2-x^2)^{1/2} , \tag{3.13}$$

where

$$R=(\epsilon_d-1)^{1/2}\frac{\omega d}{c} . \tag{3.14}$$

By combining Eqs. (3.11) and (3.13), we obtain the equation satisfied by x,

$$(R^2-x^2)^{1/2}=-x\cot x , \quad 0<x<R . \tag{3.15}$$

The solutions $\{x_n\}$ of this equation for given values of ϵ_d, ω, and d, are then substituted into the first of Eqs. (3.12) to yield the values of the wave numbers $\{q_n(\omega)\}$ of the guided-wave polaritons of frequency ω. A plot of the dispersion curves of these modes obtained in this way is presented as Fig. 3.

A graphical examination of Eq. (3.15) shows that it possesses no solution for

$$0<R<\frac{\pi}{2} , \tag{3.16a}$$

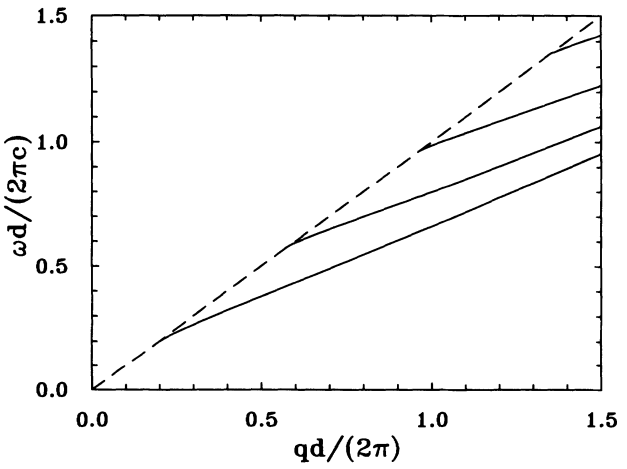

FIG. 3. Dispersion curves for s-polarized guided waves in a dielectric film of dielectric constant $\epsilon_d=2.6896$ and thickness d on a perfectly conducting substrate.

one solution for

$$\frac{\pi}{2}<R<\frac{3\pi}{2}\ , \tag{3.16b}$$

two solutions for

$$\frac{3\pi}{2}<R<\frac{5\pi}{2}\ , \tag{3.16c}$$

and, in general, p solutions for

$$(2p-1)\frac{\pi}{2}<R<(2p+1)\frac{\pi}{2}\ . \tag{3.17}$$

To simplify the discussion, in what follows we will be interested in the case in which the scattering system supports two guided waves, which can be excited through the roughness of the vacuum-film interface by an s-polarized electromagnetic wave of wavelength λ incident on it. From Eq. (3.16c), we find that this will be the case if the mean thickness of the film d satisfies the inequalities

$$\frac{3}{4(\epsilon_d-1)^{1/2}}<\frac{d}{\lambda}<\frac{5}{4(\epsilon_d-1)^{1/2}}\ . \tag{3.18}$$

IV. PERTURBATION THEORY

In this article the contribution to the mean differential reflection coefficient from the incoherent component of the scattered light will be calculated by means of a formally exact computer-simulation approach in Sec. V. To guide the computer-simulation calculations, and because it provides explicit analytic expressions from which the dominant contributions to the effect we are investigating can be obtained, we preface the exact calculations by a perturbation-theoretic calculation of the contribution to the mean differential reflection coefficient from the incoherent component of the scattered light that is valid through terms of fourth order in the surface-profile function. It has been shown in an earlier study of the enhanced backscattering of light from a one-dimensional, randomly rough, metal surface that this approximation suffices not only to predict enhanced backscattering, but also to describe the effect quantitatively.[7] We will see that the same is true in the present context as well.

A. Scattering theory

We assume that an s-polarized electromagnetic wave of frequency ω is incident from the vacuum side onto the vacuum-dielectric interface $x_3=\zeta(x_1)$. The electric vector in this case has the form given by Eq. (3.1). In the vacuum region $x_3>\zeta(x_1)_{\max}$, the field amplitude $E_2(x_1,x_3|\omega)$ is the sum of an incident wave and a scattered field

$$E_2^{>}(x_1,x_3|\omega)=\exp[ikx_1-i\alpha_0(k,\omega)x_3]+\int_{-\infty}^{\infty}\frac{dq}{2\pi}R_s(q|k)\exp[iqx_1+i\alpha_0(q,\omega)x_3]\ , \tag{4.1}$$

where

$$\alpha_0(q,\omega)=\begin{cases}[(\omega^2/c^2)-q^2]^{1/2}\ , & q^2<\omega^2/c^2 \quad (4.2a)\\ i[q^2-(\omega^2/c^2)]^{1/2}\ , & q^2>\omega^2/c^2\ . \quad (4.2b)\end{cases}$$

Within the film, $-d<x<\zeta(x_1)$, $E_2(x_1,x_3|\omega)$ has the form

$$E_2^{<}(x_1,x_3|\omega)=\int_{-\infty}^{\infty}\frac{dq}{2\pi}T_s(q|k)\exp[iqx_1]\sin\alpha_d(q,\omega)(x_3+d)\ , \tag{4.3}$$

where

$$\alpha_d(q,\omega)=\begin{cases}[\epsilon_d(\omega^2/c^2)-q^2]^{1/2}\ , & q^2<\epsilon_d(\omega^2/c^2) \quad (4.4a)\\ i[q^2-\epsilon_d(\omega^2/c^2)]^{1/2}\ , & q^2>\epsilon_d(\omega^2/c^2)\ . \quad (4.4b)\end{cases}$$

The contribution to the mean differential reflection coefficient from the light scattered incoherently is given in terms of the scattering amplitude $R_s(q|k)$ by

$$\left\langle\frac{\partial R_s}{\partial\theta_s}\right\rangle_{\text{incoh}}=\frac{1}{L_1}\frac{\omega}{2\pi c}\frac{\cos^2\theta_s}{\cos\theta_0}[\langle|R_s(q|k)|^2\rangle-|\langle R_s(q|k)\rangle|^2]\ , \tag{4.5}$$

where L_1 is the length of the mean surface $x_3=0$ in the x_1 direction, and we have introduced the angle of incidence θ_0 and the scattering angle θ_s, both measured from the normal to the mean surface, by

$$k=(\omega/c)\sin\theta_0\ ,\quad q=(\omega/c)\sin\theta_s\ . \tag{4.6}$$

By imposing the requirement that the electric-field amplitudes given by Eqs. (4.1) and (4.3) satisfy the boundary conditions at the rough vacuum-dielectric interface, we obtain the following coupled integral equations for the scattering and transmissions amplitudes $R_s(q|k)$ and $T_s(q|k)$:

$$e^{ikx_1-i\alpha_0(k,\omega)\zeta(x_1)}+\int_{-\infty}^{\infty}\frac{dq}{2\pi}R_s(q|k)e^{iqx_1+i\alpha_0(q,\omega)\zeta(x_1)}=\int_{-\infty}^{\infty}\frac{dq}{2\pi}T_s(q|k)e^{iqx_1}\sin\alpha_d(q,\omega)[\zeta(x_1)+d]\ . \tag{4.7a}$$

$$[\alpha_0(k,\omega)+k\zeta'(x_1)]e^{ikx_1-i\alpha_0(k,\omega)\zeta(x_1)}-\int_{-\infty}^{\infty}\frac{dq}{2\pi}R_s(q|k)e^{iqx_1}[\alpha_0(q,\omega)-q\zeta'(x_1)]e^{iqx_1+i\alpha_0(q,\omega)\zeta(x_1)}$$
$$=-\frac{1}{2i}\int_{-\infty}^{\infty}\frac{dq}{2\pi}T_s(q|k)\{[\alpha_d(q,\omega)-q\zeta'(x_1)]e^{iqx_1}e^{i\alpha_d(q,\omega)[\zeta(x_1)+d]}+[\alpha_d(q,\omega)+q\zeta'(x_1)]e^{iqx_1}e^{-i\alpha_d(q,\omega)[\zeta(x_1)+d]}\}\ . \tag{4.7b}$$

The assumption that the field amplitude given by Eq. (4.1) which, strictly speaking, is valid only for $x_3>\zeta(x_1)_{\max}$, can

be continued in to the surface $x_3=\zeta(x_1)$ and used in satisfying the boundary conditions there, constitutes the Rayleigh hypothesis.[8,9]

The Eqs. (4.7a) and (4.7b) can be decoupled to yield a single integral equation for the scattering amplitude $R_s(q|k)$ alone. By multiplying Eqs. (4.7a) and (4.7b) by the factors

$$e^{-ipx_1}[e^{i\alpha_d(p,\omega)[\zeta(x_1)+d]}[\alpha_d(p,\omega)+p\zeta'(x_1)]+e^{-i\alpha_d(p,\omega)[\zeta'(x_1)+d]}[\alpha_d(p,\omega)-p\zeta'(x_1)]\ ,$$

and

$$e^{-ipx_1}[e^{i\alpha_d(p,\omega)[\zeta(x_1)+d]}-e^{-i\alpha_d(p,\omega)[\zeta(x_1)+d]}]\ ,$$

respectively, integrating both with respect to x_1, and adding the resulting equations, we obtain the equation satisfied by $R_s(q|k)$

$$\int_{-\infty}^{\infty}\frac{dq}{2\pi}M(p|q)R_s(q|k)=N(p|k)\ . \tag{4.8}$$

The functions $M(p|q)$ and $N(p|k)$ appearing in Eq. (4.8) are given by

$$M(p|q)=\frac{e^{i\alpha_d(p,\omega)d}}{\alpha_0(q,\omega)+\alpha_d(p,\omega)}I[\alpha_0(q,\omega)+\alpha_d(p,\omega)|p-q]-\frac{e^{-i\alpha_d(p,\omega)d}}{\alpha_0(q,\omega)-\alpha_d(p,\omega)}I[\alpha_0(q,\omega)-\alpha_d(p,\omega)|p-q]\ , \tag{4.9}$$

$$N(p|k)=-\frac{e^{i\alpha_d(p,\omega)d}}{\alpha_d(p,\omega)-\alpha_0(k,\omega)}I[\alpha_d(p,\omega)-\alpha_0(k,\omega)|p-k]-\frac{e^{-i\alpha_d(p,\omega)d}}{\alpha_d(p,\omega)+\alpha_0(k,\omega)}I[-\alpha_d(p,\omega)-\alpha_0(k,\omega)|p-k]\ , \tag{4.10}$$

where

$$I(\gamma|Q)=\int_{-\infty}^{\infty}dx_1e^{-iQx_1}e^{i\gamma\zeta(x_1)}\ . \tag{4.11}$$

Equations (4.8)–(4.11) constitute the basis of our perturbation-theoretic analysis. We seek $R_s(q|k)$ as an expression in powers of the surface-profile function, in the form

$$R_s(q|k)=\sum_{n=0}^{\infty}\frac{1}{n!}R_s^{(n)}(q|k)\ , \tag{4.12}$$

where the superscript denotes the order of the corresponding term in $\zeta(x_1)$. We also expand $M(p|q)$, $N(p|k)$, and $I(\gamma|Q)$ in a similar fashion

$$M(p|q)=\sum_{n=0}^{\infty}\frac{1}{n!}M^{(n)}(p|q)\ , \tag{4.13}$$

$$N(p|k)=\sum_{n=0}^{\infty}\frac{1}{n!}N^{(n)}(p|k)\ , \tag{4.14}$$

$$I(\gamma|Q)=\sum_{n=0}^{\infty}\frac{(i\gamma)^n}{n!}\hat{\zeta}^{(n)}(Q)\ , \tag{4.15}$$

where

$$\hat{\zeta}^{(n)}(Q)=\int_{-\infty}^{\infty}dx_1e^{-Qx_1}\zeta^n(x_1)\ . \tag{4.16}$$

By substituting Eqs. (4.12)–(4.15) into Eq. (4.8), and then equating in the resulting equation terms of the same order in $\zeta(x_1)$, we are led to the following recurrence relation for the $\{R_s^{(n)}(q|k)\}$:

$$M^{(0)}(p,\omega)R_s^{(0)}(p|k)=2\pi\delta(p-k)N^{(0)}(k,\omega)\ , \tag{4.17a}$$

$$M^{(0)}(p,\omega)R_s^{(n)}(p|k)=N^{(n)}(p|k)-\int_{-\infty}^{\infty}\frac{dq}{2\pi}M^{(n)}(p|q)R_s^{(0)}(q|k)-\sum_{r=1}^{n-1}\binom{n}{r}\int_{-\infty}^{\infty}\frac{dq}{2\pi}M^{(n-r)}(p|q)R_s^{(r)}(q|k)\ ,$$

$$n\geq 1\ , \tag{4.17b}$$

where we have used the results that

$$M^{(0)}(p|q)=2\pi\delta(p-q)M^{(0)}(p,\omega)\ , \tag{4.18}$$

$$N^{(0)}(p|k)=2\pi\delta(p-k)N^{(0)}(k,\omega)\ , \tag{4.19}$$

with

$$M^{(0)}(p,\omega)=-\frac{2i}{\epsilon_d-1}\frac{c^2}{\omega^2}D_+(p,\omega)\ , \tag{4.20}$$

$$N^{(0)}(k,\omega)=-\frac{2i}{\epsilon_d-1}\frac{c^2}{\omega^2}D_-(k,\omega)\ , \tag{4.21}$$

and

$$D_\pm(k,\omega)=\alpha_0(k,\omega)\sin\alpha_d(k,\omega)d\pm i\alpha_d(k,\omega)\cos\alpha_d(k,\omega)d\ . \tag{4.22}$$

From Eqs. (4.9)–(4.11) and (4.13)–(4.16) we obtain the terms in the expansions of $M(p|q)$ and $N(p|k)$ for $n\geq 1$

$$M^{(n)}(p|q)=i^n\{e^{i\alpha_d(p,\omega)d}[\alpha_0(q,\omega)+\alpha_d(p,\omega)]^{n-1} - e^{-i\alpha_d(p,\omega)d}[\alpha_0(q,\omega) -\alpha_d(p,\omega)]^{n-1}\}\hat{\xi}^{(n)}(p-q) , \tag{4.23}$$

$$N^{(n)}(p|k)=-i^n\{e^{i\alpha_d(p,\omega)d}[\alpha_d(p,\omega)-\alpha_0(k,\omega)]^{n-1} + e^{-i\alpha_d(p,\omega)d}[\alpha_d(p,\omega) -\alpha_0(k,\omega)]^{n-1}\}\hat{\xi}^{(n)}(p-k) . \tag{4.24}$$

We can now use the recurrence relation, Eqs. (4.17), together with Eqs. (4.20)–(4.24), to calculate $R_s(p|k)$ up to the desired order in its expansion in powers of $\zeta(x_1)$ [Eq. (4.12)]. For our purpose, it suffices to obtain the four leading terms, which are given by

$$R_s^{(0)}(p|k)=2\pi\delta(p-k)\frac{D_-(k,\omega)}{D_+(k,\omega)} \equiv 2\pi\delta(p-k)R_s^{(0)}(k,\omega) , \tag{4.25}$$

$$R_s^{(1)}(p|k)=iu_1(\omega)\hat{\xi}^{(1)}(p-k) \times\frac{\sin\alpha_d(p,\omega)d}{D_+(p,\omega)}\frac{2\alpha_0(k,\omega)\sin\alpha_d(k,\omega)d}{D_+(k,\omega)} , \tag{4.26}$$

$$R_s^{(2)}(p|k)=iu_1(\omega)\frac{\sin\alpha_d(p,\omega)d}{D_+(p,\omega)}\left\{\hat{\xi}^{(2)}(p-k)[\alpha_d(p,\omega)\cot\alpha_d(p,\omega)d+\alpha_d(k,\omega)\cot\alpha_d(k,\omega)d] +2iu_1(\omega)\int_{-\infty}^{\infty}\frac{dq}{2\pi}\hat{\xi}^{(1)}(p-q)\frac{\sin\alpha_d(q,\omega)d}{D_+(q,\omega)}\hat{\xi}^{(1)}(q-k)\right\}\frac{2\alpha_0(k,\omega)\sin\alpha_d(k,\omega)d}{D_+(k,\omega)} , \tag{4.27}$$

$$\begin{aligned}R_s^{(3)}(p|k)=iu_1(\omega)\frac{\sin\alpha_d(p,\omega)d}{D_+(p,\omega)}\Bigg\{&\hat{\xi}^{(3)}(p-k)\left[(2-4\epsilon_d)\frac{\omega^2}{c^2}+p^2+k^2+2\alpha_d(p,\omega)\alpha_d(k,\omega)\cot\alpha_d(p,\omega)d\cot\alpha_d(k,\omega)d\right]\\ &+3iu_1(\omega)\int_{-\infty}^{\infty}\frac{dq}{2\pi}[\alpha_d(p,\omega)\cot\alpha_d(p,\omega)d+\alpha_d(q,\omega)\cot\alpha_d(q,\omega)d]\\ &\times\hat{\xi}^{(2)}(p-q)\frac{\sin\alpha_d(q,\omega)d}{D_+(q,\omega)}\hat{\xi}^{(1)}(q-k)\\ &+3iu_1(\omega)\int_{-\infty}^{\infty}\frac{dq}{2\pi}\hat{\xi}^{(1)}(p-q)\frac{\sin\alpha_d(q,\omega)d}{D_+(q,\omega)}[\alpha_d(q,\omega)\cot\alpha_d(q,\omega)d\\ &+\alpha_d(k,\omega)\cot\alpha_d(k,\omega)d]\hat{\xi}^{(2)}(q-k)\\ &-6[u_1(\omega)]^2\int_{-\infty}^{\infty}\frac{dq}{2\pi}\int_{-\infty}^{\infty}\frac{dr}{2\pi}\hat{\xi}^{(1)}(p-q)\frac{\sin\alpha_d(q,\omega)d}{D_+(q,\omega)}\hat{\xi}^{(1)}(q-r)\\ &\times\frac{\sin\alpha_d(r,\omega)d}{D_+(r,\omega)}\hat{\xi}^{(1)}(r-k)\Bigg\}\frac{2\alpha_0(k,\omega)\sin\alpha_d(k,\omega)d}{D_+(k,\omega)} ,\end{aligned} \tag{4.28}$$

where

$$u_1(\omega)\equiv(\epsilon_d-1)\frac{\omega^2}{c^2} . \tag{4.29}$$

Upon substituting these four terms into Eq. (4.5) and keeping terms up to fourth order in $\zeta(x_1)$ in the resulting equation, one can readily obtain the contribution to the mean differential reflection coefficient from the light scattered incoherently up to the same order in $\zeta(x_1)$. In doing so, we explicitly take into account the statistical properties of the Gaussian stochastic process $\zeta(x_1)$ as stated in Sec. II, thus arriving at

$$\left\langle\frac{\partial R_s}{\partial\theta_s}\right\rangle_{\text{incoh}}=\frac{2}{\pi}\left[\frac{\omega}{c}\right]^3\cos^2\theta_s\cos\theta_0|G_0(p,\omega)|^2\{I_2(p|k)+I_4^{(2-2)L}(p|k)+I_4^{(2-2)C}(p|k)+I_4^{(1-3)}(p|k)\}|G_0(k,\omega)|^2 . \tag{4.30}$$

The functions appearing in this expression are given by

$$I_2(p|k)=\delta^2[u_1(\omega)]^2g(|p-k|) , \tag{4.31}$$

$$I_4^{(2-2)L}(p|k)=\delta^4\int_{-\infty}^{\infty}\frac{dq}{2\pi}g(|p-q|)g(|q-k|)\{|u_1(\omega)u_2(p|k)|^2+2\,\mathrm{Re}\{[u_1(\omega)]^3u_2(p|k)G_0^*(q,\omega)\}$$
$$+[u_1(\omega)]^4|G_0(q,\omega)|^2\}\ , \tag{4.32}$$

$$I_4^{(2-2)C}(p|k)=\delta^4\int_{-\infty}^{\infty}\frac{dq}{2\pi}g(|p-q|)g(|q-k|)\{|u_1(\omega)u_2(p|k)|^2+2\,\mathrm{Re}\{[u_1(\omega)]^3u_2(p|k)G_0^*(q,\omega)\}$$
$$+[u_1(\omega)]^4G_0(q,\omega)G_0^*(p+k-q,\omega)\}\ , \tag{4.33}$$

$$I_4^{(1-3)}(p|k)=2\delta^4g(|p-k|)\mathrm{Re}\Big\{3u_1(\omega)u_3(p|k)+[u_1(\omega)]^3[u_2(k|k)G_0(k,\omega)+u_2(p|p)G_0(p,\omega)]$$
$$+2[u_1(\omega)]^3\int_{-\infty}^{\infty}\frac{dq}{2\pi}[g(|p-q|)u_2(q|k)+g(|q-k|)u_2(p|q)]G_0(q,\omega)$$
$$+[u_1(\omega)]^4\int_{-\infty}^{\infty}\frac{dq}{2\pi}G_0(q,\omega)\{g(|p-q|)[G_0(p,\omega)+\tfrac{1}{2}G_0(k-p+q,\omega)]$$
$$+g(|q-k|)[G_0(k,\omega)+\tfrac{1}{2}G_0(p-k+q,\omega)]\}\Big\}\ , \tag{4.34}$$

where $u_1(\omega)$ is given by Eq. (4.29), and

$$u_2(p|k)=\tfrac{1}{2}[\alpha_d(p,\omega)\cot\alpha_d(p,\omega)d$$
$$+\alpha_d(k,\omega)\cot\alpha_d(k,\omega)d]\ , \tag{4.35}$$

$$u_3(p|k)=\frac{u_1(\omega)}{6}\Big[(p^2+k^2)-(4\epsilon_d-2)\frac{\omega^2}{c^2}$$
$$+2\alpha_d(p,\omega)\alpha_d(k,\omega)\cot\alpha_d(p,\omega)d$$
$$\times\cot\alpha_d(k,\omega)d\Big]\ , \tag{4.36}$$

while $G_0(p,\omega)$ is the Green's function for the planar vacuum-dielectric interface,

$$G_0(p,\omega)\equiv\frac{i\sin\alpha_d(p,\omega)d}{D_+(p,\omega)}\ . \tag{4.37}$$

$I_2(p|k)$ gives the contribution to Eq. (4.30) of second order in $\zeta(x_1)$, whereas $I_4^{(2-2)L}$, $I_4^{(2-2)C}$, and $I_4^{(1-3)}$, yield the contributions of fourth order in $\zeta(x_1)$ from, respectively, the ladder term, the maximally crossed term, and the contribution consisting of products of terms in $R_s(p|k)$ of first and third orders in $\zeta(x_1)$.

It should be noted that, in obtaining Eqs. (4.30)–(4.37) in the form shown above, we have made use of a reformulation of the problem by means of a scattering theory that manifestly ensures the reciprocity and the unitarity of the scattering process. This formulation is addressed in the Appendix.

B. Numerical results

We will evaluate the result for $\langle\partial R_s/\partial\theta_s\rangle_{\mathrm{incoh}}$ obtained in Sec. IV A for a dielectric film whose dielectric constant is $\epsilon_d=2.6896+i0.0075$, deposited on a perfectly conducting substrate. The small imaginary part of the dielectric constant has been introduced to yield a finite width to each of the peaks in $\langle\partial R_s/\partial\theta_s\rangle_{\mathrm{incoh}}$. The vacuum-dielectric interface is a one-dimensional random interface as described in Sec. II, whose roughness parameters are $a=100$ nm and $\delta=15$ nm. An s-polarized plane wave of wavelength $\lambda=632.8$ nm is incident on it from the vacuum side. With these choices of the roughness parameters the usual conditions for the validity of small-amplitude perturbation theory in application to rough surface scattering,[10] viz., $\delta/\lambda\ll1$ and $\delta/a\ll1$, are well satisfied. The thickness of the film is chosen in such a way that the corresponding planar dielectric film supports only two guided-wave polaritons at the frequency ω, in accordance with the discussion in Sec. III. In light of the dispersion curves shown in Fig. 3, we assume $d=500$ nm, so that the wave vectors of the two guided-wave polaritons are $q_1(\omega)=(\omega/c)\ 1.5466$ and $q_2(\omega)=(\omega/c)\ 1.2423$.

We have numerically evaluated the contribution to the mean differential reflection coefficient from the incoherent component of the scattered light through terms of fourth order in $\zeta(x_1)$ [Eqs. (4.30)–(4.37)] as a function of the scattering angle θ_s for the parameters given above, for a few different angles of incidence θ_0. The result for normal incidence is shown in Fig. 4. The contributions arising from the second-order term [Eq. (4.31)] and the fourth-order term [Eqs. (4.32)–(4.34)] are plotted separately. In addition to the well-known, strong, enhanced backscattering peak, two small satellite peaks symmetrically placed with respect to $\theta_s=0°$ at $\theta_\pm=\pm17.7°$ are also observed in the fourth-order contribution. In Fig. 5, we split this fourth-order term into its three separate contributions: the ladder term $(2\text{-}2)_L$ [Eq. (4.32)], the crossed term $(2\text{-}2)_C$ [Eq. (4.33)], and the (1-3) term [Eq. (4.34)]. In light of the results shown in Fig. 5, it is evident that the enhanced backscattering peak and the satellite peaks originate entirely in the fourth-order crossed contribution. As we mentioned in the preceding section, this term contains information about the interference effects between every doubly scattered light path and its time-reversed partner, a phenomenon that we believe underlies the existence of such peaks. In fact, the simple argument that takes into account the phases of such trajectories resulting from the interplay of the two guided waves and leads to Eq. (1.1) in the case of an arbitrary number of

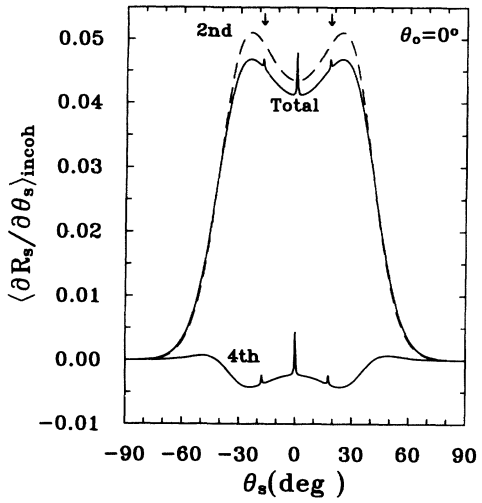

FIG. 4. Contribution through fourth order in the surface-profile function to the mean differential reflection coefficient from the incoherent component of the scattered light for s-polarized light of wavelength $\lambda=632.8$ nm incident at $\theta_0=0°$ on a dielectric film of mean thickness $d=500$ nm and dielectric constant $\epsilon_d=2.6896+i0.0075$, deposited on a planar perfectly conducting substrate. The one-dimensional, randomly rough, vacuum-dielectric interface is characterized by the parameters $\delta=15$ nm and $a=100$ nm. The second-order and fourth-order contributions are included also.

guided waves, predicts that the two satellite peaks should occur at scattering angles $\theta_\pm$ given by

$$\sin\theta_\pm=-\sin\theta_0\pm(c/\omega)[q_1(\omega)-q_2(\omega)]\ . \tag{4.38}$$

Note that, when $q_1(\omega)=q_2(\omega)$, Eq. (4.38) yields the direction of the enhanced backscattering peak, as expected. In Figs. 4 and 5 these two angles are marked by arrows and coincide accurately with the positions of the peaks obtained through the perturbation-theoretic calculations ($\theta_\pm=\pm17.7°$).

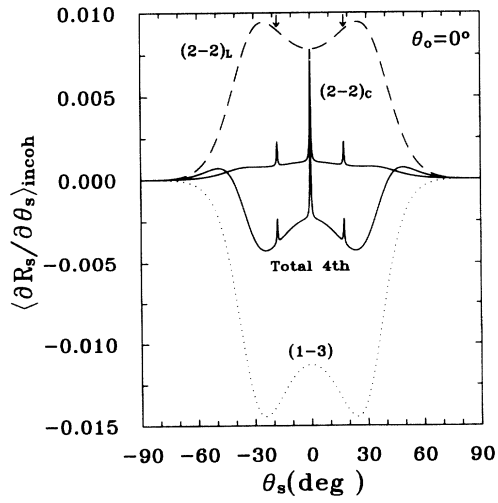

FIG. 5. Same as Fig. 3 but only for the fourth-order contribution, including separately the ladder, crossed, and (1-3) terms.

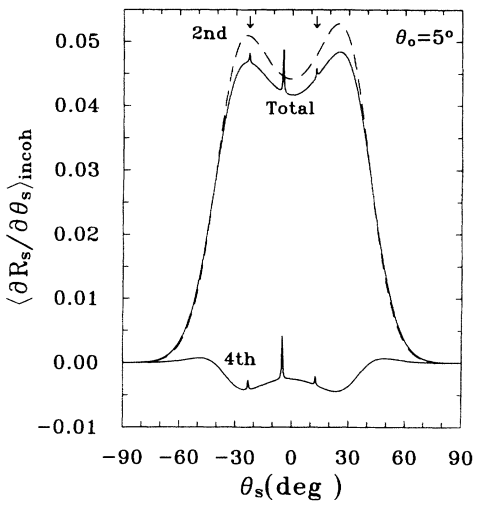

FIG. 6. Same as Fig. 4 but for $\theta_0=5°$.

In order to demonstrate the displacement of the satellite peaks as the angle of incidence is varied, we show in Figs. 6 and 7 the numerical results of the perturbation theory for the case considered in obtaining Figs. 4 and 5, respectively, but for $\theta_0=5°$. As expected, Fig. 6 reveals two peaks about the backscattering peak at $\theta_-=12.6°$, and $\theta_-=-23.1°$, whose positions, precisely determined by the conditions (4.38), are indicated by arrows. Figure 7 confirms that those peaks and the backscattering peak stem from the fourth-order crossed contribution, as expected.

It is important to note that the total contribution of fourth order in $\zeta(x_1)$ is sufficiently smaller than the contribution of second order in $\zeta(x_1)$ (see Figs. 4 and 6) that the use of perturbation theory for the calculation of $\langle \partial R_s/\partial \theta_s \rangle_{incoh}$ should be valid for the roughness parameters assumed.

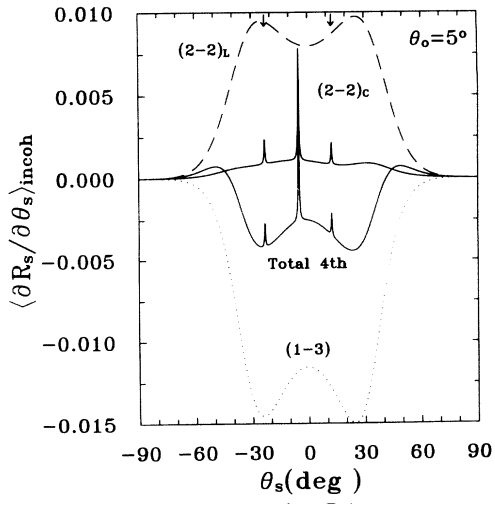

FIG. 7. Same as Fig. 5 but for $\theta_0=5°$.

V. NUMERICAL SIMULATION RESULTS

We have also carried out numerical simulations of the scattering of s-polarized light from the structure depicted in Fig. 2. In these simulations the incident light was represented by a beam of finite width, and the surface-profile function $\zeta(x_1)$ was assumed to possess the statistical properties described in Sec. II. The calculations were carried out on the basis of the equations derived in detail in Ref. 11. The wavelength of the incident light was taken to be $\lambda=632.8$ nm and the dielectric constant of the film at this wavelength was assumed to be $\epsilon_d=2.6896$, which is the value appropriate to photoresist. In order that the scattering structure support only two guided-wave polaritons for these values of λ and ϵ_d in the absence of the surface roughness, we find from Eq. (3.18) that the mean thickness of the film d has to satisfy the inequalities 365.1 nm $< d <$ 608.5 nm.

The length L of the rough surfaces used in the simulations was $L=25\,600$ nm. The ratio L/g assumed in this work, where g is the half-width of the intercept of the incident beam with the mean scattering plane $x_3=0$, was $L/g=4$. The length L was divided into $N=400$ subintervals of equal length in solving the integral equations arising in the scattering theory presented in Ref. 11 by converting them into matrix equations. In the calculation of the contribution to the mean differential reflection coefficient from the incoherent component of the scattered light, $\langle \partial R_s/\partial\theta_s \rangle_{\text{incoh}}$ averages over $N_p=1000$ realizations of the surface profile, generated by the method described in Appendix A of Ref. 12, were used.

The angle of incidence assumed in these calculations was fixed at $\theta_0=0°$, i.e., normal incidence was assumed, and the mean thickness d of the dielectric film was varied. This choice of experimental conditions was made because in the numerical simulations, which take multiple-scattering of all orders into account, it was found that as the angle of incidence is given increasing positive values, the satellite peak at the scattering angle $\theta_s=\theta_-$, which is the larger of the two angles $\theta_\pm$ in magnitude, washes out rapidly, presumably due to shadowing effects, and only the satellite peak at $\theta_s=\theta_+$ is observed. At normal incidence both satellite peaks are clearly visible in $\langle \partial R_s/\partial\theta_s \rangle_{\text{incoh}}$, and as the thickness of the film is decreased, the scattering angles $\theta_s=\theta_+=-\theta_-$ at which they occur increase in magnitude due to the changes in the values of the wave numbers $q_1(\omega)$ and $q_2(\omega)$ entering Eq. (4.38). In our calculations values of d equal to 580 and 500 nm were used. The satellite peaks for these choices of d should occur at scattering angles given by $\theta_s=\pm 13.3°$ and $\theta_s=\pm 17.7°$, respectively.

In Fig. 8 we present our results in the case that the surface roughness is characterized by the parameters $\delta=110$ nm and $a=260$ nm. For a mean film thickness of $d=580$ nm [Fig. 8(a)], in addition to the enhanced backscattering peak at $\theta_s=0°$ two well-defined satellite peaks, symmetrically placed with respect to the retroreflection direction, are observed. The vertical dashed lines indicate the positions of the satellite peaks predicted by Eq. (4.38). When the thickness of the film is decreased to 500 nm [Fig. 8(b)], the positions of the two satellite peaks are shifted to larger values of the scattering angle as expected. The small differences between the values of the scattering angles at which the satellite peaks occur in the numerical-simulation results and the values predicted by Eq. (4.38) are presumably due to the fact that the numerical simulations take into account the renormalization of the values of $q_1(\omega)$ and $q_2(\omega)$ caused by the surface roughness, while the values of $q_1(\omega)$ and $q_2(\omega)$ used in obtaining the predicted values of $\theta_\pm$ were calculated in the absence of the roughness.

We also note that the angular width of the enhanced backscattering peak, as defined by the distance between

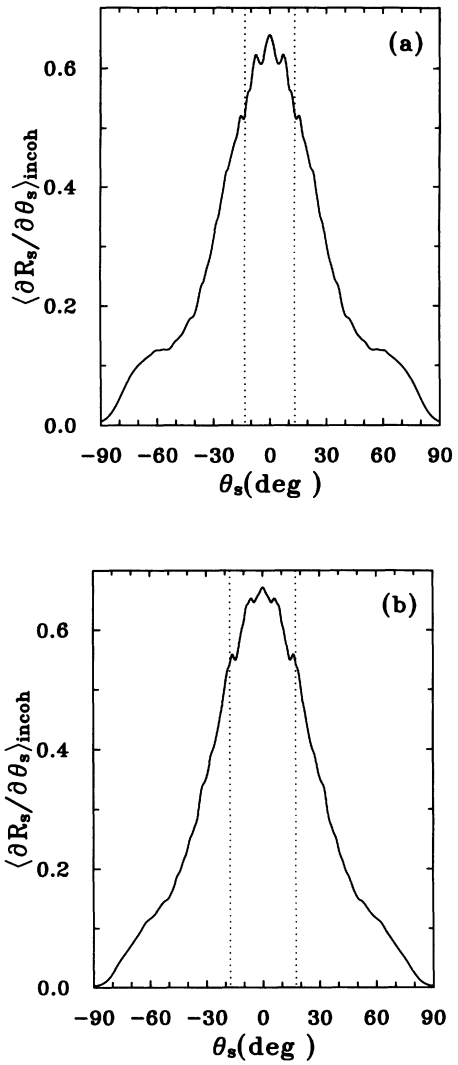

FIG. 8. Computer-simulation results for the differential reflection coefficient $\langle \partial R_s/\partial\theta_s \rangle_{\text{incoh}}$ for the scattering of a s-polarized beam of light from a one-dimensional random surface on a photoresist film deposited on a planar perfectly conducting substrate. $\theta_0=0°$, $\delta=110$ nm, $a=260$ nm, $\lambda=632.8$ nm, $\epsilon_d=2.6896$, $L=25\,600$ nm, $g=6400$ nm, $N=400$, $N_p=1000$. (a) $d=580$ nm, (b) $d=500$ nm. The vertical dashed lines indicate the scattering angles at which the satellite peaks should occur according to Eq. (4.38).

the subsidiary minima separating the subsidiary maxima from the enhanced backscattering peak, does not change when d is changed. This is as expected, since the angular width of the enhanced backscattering peak is determined by the ratio λ/a[13], and thus should not change when only d is changed.

VI. CONCLUSIONS

In conclusion, we note that the results obtained in this paper for the angular dependence of the intensity of the light that has been scattered diffusely from a thin dielectric film with a one-dimensional, randomly rough interface with vacuum deposited on the planar surface of a perfect conductor, which supports two guided-wave modes, have qualitatively the same structure for any other bounded system with a discrete spectrum, independently of the nature of the scatterers (volume or surface), the transverse dimension of the system (film thickness), and the nature of the modes comprising the discrete spectrum. The sole requirement for obtaining such a dependence is that the mean free paths of these modes must be much larger than the inverse of the characteristic "distance" between the wave numbers of consecutive modes $\delta q(\omega) \simeq |q_{n+1}(\omega) - q_n(\omega)|$. When this condition is satisfied, enhanced scattering occurs not only into the retroreflection direction, but also into additional scattering directions. The number of the additional, satellite, peaks is determined by the number of discrete guided modes supported by the scattering system, and the amplitudes of the peaks are inversely proportional to the thickness of the film.[6]

ACKNOWLEDGMENTS

This work was supported in part by the United States–Israel Binational Science Foundation Grant No. 92-00248, and by Army Research Office Grant No. DAAL03-92-G-0239. It was also supported by the University of California, Irvine, through an allocation of computer time. J.A.S.G. acknowledges a grant from the Consejo Superior de Investigaciones Científicas.

APPENDIX

In this Appendix we sketch out the manner in which the low-order perturbative calculation described in Sec. IV can be related to the kind of many-body perturbation theory calculation employed by Freilikher, Pustilnik, and Yurkevich[6] in their general treatment of the scattering of light by random systems displaying degenerate time-reversal symmetry.

We begin by postulating that the scattering amplitude $R_s(q|k)$ has the form[14]

$$R_s(q|k) = 2\pi\delta(q-k)R_0(k,\omega) - 2iG_0(q,\omega)T(q|k)G_0(k,\omega)\alpha_0(k,\omega) . \quad \text{(A1)}$$

In this expression $R_0(k,\omega)$ is the Fresnel coefficient for the scattering of s-polarized light from a dielectric film deposited on a perfectly conducting substrate, when the vacuum-dielectric and dielectric-substrate interfaces are planar and parallel. It is given by Eq. (4.25) as

$$R_0(k,\omega) = \frac{-i\alpha_d(k,\omega)\cos\alpha_d(k,\omega)d + \alpha_0(k,\omega)\sin\alpha_d(k,\omega)d}{i\alpha_d(k,\omega)\cos\alpha_d(k,\omega)d + \alpha_0(k,\omega)\sin\alpha_d(k,\omega)d} . \quad \text{(A2)}$$

The function $G_0(k,\omega)$ is a Green's function for the same dielectric film on a perfectly conducting substrate system, and the transition matrix $T(q|k)$ is postulated to satisfy the equations

$$T(q|k) = V(q|k) + \int_{-\infty}^{\infty} \frac{dp}{2\pi} V(q|p)G_0(p,\omega)T(p|k) \quad \text{(A3a)}$$

$$= V(q|k) + \int_{-\infty}^{\infty} \frac{dp}{2\pi} T(q|p)G_0(p,\omega)V(p|k) , \quad \text{(A3b)}$$

where the scattering potential $V(q|k)$ is defined by Eqs. (4.8), (A1) and (A3) once we know what $G_0(k,\omega)$ is. We also introduce the Green's function $G(q|k)$ for the dielectric film on a perfectly conducting substrate in the case that the vacuum-dielectric interface is no longer planar but is defined by the equation $x_3 = \zeta(x_1)$. It is the solution of the equation

$$G(q|k) = 2\pi\delta(q-k)G_0(k,\omega) + G_0(q,\omega)\int_{-\infty}^{\infty} \frac{dp}{2\pi} V(q|p)G(p|k) \quad \text{(A4a)}$$

$$= 2\pi\delta(q-k)G_0(k,\omega) + G_0(q,\omega)T(q|k)G_0(k,\omega) . \quad \text{(A4b)}$$

When we use Eq. (A4b) in Eq. (A1), we find that the scattering amplitude $R_s(q|k)$ takes the form

$$R_s(q|k) = 2\pi\delta(q-k)[R_0(k,\omega) + 2i\alpha_0(k,\omega)G_0(k,\omega)] - 2iG(q|k)\alpha_0(k,\omega) . \quad \text{(A5)}$$

We now use the preceding results to obtain $G_0(k,\omega)$ and $V(q|k)$.

We first define $G_0(k,\omega)$ through the condition

$$R_0(k,\omega) + 2i\alpha_0(k,\omega)G_0(k,\omega) = -1 , \quad \text{(A6)}$$

which yields the result that

$$G_0(k,\omega) = \frac{i\sin\alpha_d(k,\omega)d}{i\alpha_d(k,\omega)\cos\alpha_d(k,\omega)d + \alpha_0(k,\omega)\sin\alpha_d(k,\omega)d} . \quad \text{(A7)}$$

The motivation for this choice is that it reduces the expression (A5) for the scattering amplitude to the simple form

$$R_s(q|k) = -2\pi\delta(q-k) - 2iG(q|k)\alpha_0(k,\omega) . \quad \text{(A8)}$$

By combining Eq. (A8) with Eq. (4.5) we find that the contribution to the mean differential reflection coefficient from the incoherent component of the scattered light is given in terms of the Green's function $G(q|k)$ by

$$\left\langle \frac{\partial R_s}{\partial \theta_s} \right\rangle_{\text{incoh}} = \frac{1}{L_1}\frac{2}{\pi}\left[\frac{\omega}{c}\right]^3 \cos^2\theta_s \cos\theta_0 \times [\langle |G(q|k)|^2\rangle - |\langle G(q|k)\rangle|^2] , \quad \text{(A9)}$$

where $q=(\omega/c)\sin\theta_s$ and $k=(\omega/c)\sin\theta_0$.

If we substitute Eq. (A1) into Eq. (4.8), we obtain an equation satisfied by the transition matrix $T(q|k)$,

$$\int_{-\infty}^{\infty}\frac{dq}{2\pi}M(p|q)G_0(q,\omega)T(q|k) = \frac{[M(p|k)R_0(k,\omega)-N(p|k)]}{2i\alpha_0(k,\omega)G_0(k,\omega)} . \quad \text{(A10)}$$

If $T(q|k)$ in this equation is now replaced by the right-hand side of Eq. (A3b), the result is

$$\int_{-\infty}^{\infty}\frac{dq}{2\pi}M(p|q)G_0(q,\omega)V(q|k)+\int_{-\infty}^{\infty}\frac{dq}{2\pi}\int_{-\infty}^{\infty}\frac{dr}{2\pi}M(p|q)G_0(q,\omega)T(q|r)G_0(r,\omega)V(r|k) = \frac{[M(p|k)R_0(k,\omega)-N(p|k)]}{2i\alpha_0(k,\omega)G_0(k,\omega)} . \quad \text{(A11)}$$

If we use Eq. (A10) in the second term on the left-hand side of Eq. (A11) to eliminate $T(q|r)$, we obtain finally the equation satisfied by the scattering potential $V(q|k)$,

$$\int_{-\infty}^{\infty}\frac{dq}{2\pi}[M(p|q)+N(p|q)]\frac{V(q|k)}{2i\alpha_0(q,\omega)} = \frac{[M(p|k)D_-(k,\omega)-N(p|k)D_+(k,\omega)]}{2\alpha_0(k,\omega)\sin\alpha_d(k,\omega)d} , \quad \text{(A12)}$$

where we have used Eq. (A6) to simplify the left-hand side.

We can solve Eq. (A12) for $V(q|k)$ as an expansion in powers of the surface-profile function $\zeta(x_1)$. Thus, if we write

$$V(q|k)=\sum_{n=1}^{\infty}V^{(n)}(q|k) , \quad \text{(A13)}$$

where the superscript denotes the order of the corresponding term in $\zeta(x_1)$, we obtain for the first three terms in this expansion

$$V^{(1)}(q|k)=(\epsilon_d-1)\frac{\omega^2}{c^2}\hat{\zeta}^{(1)}(q-k) , \quad \text{(A14a)}$$

$$V^{(2)}(q|k)=\tfrac{1}{2}(\epsilon_d-1)\frac{\omega^2}{c^2}\hat{\zeta}^{(2)}(q-k)[\alpha_d(q,\omega)\cot\alpha_d(q,\omega)d+\cot\alpha_d(k,\omega)d\alpha_d(k,\omega)] , \quad \text{(A14b)}$$

$$V^{(3)}(q|k)=\tfrac{1}{6}(\epsilon_d-1)\frac{\omega^2}{c^2}[q^2+k^2-(4\epsilon_d-2)\frac{\omega^2}{c^2}+2\alpha_d(q,\omega)\cot\alpha_d(q,\omega)d\,\cot\alpha_d(k,\omega)d\alpha_d(k,\omega)]\hat{\zeta}^{(3)}(q-k) . \quad \text{(A14c)}$$

In the small roughness approximation the scattering potential $V(q|k)$ in Eqs. (A3) and (A4a) is approximated by $V^{(1)}(q|k)$, given by Eq. (A14a). We will make this approximation in what follows.

The calculation of the contribution to the mean differential reflection coefficient from the incoherent component of the scattered field, Eq. (A9), requires knowledge of the averaged Green's function $\langle G(q|k)\rangle$. Due to the stationarity of the surface-profile function $\zeta(x_1)$, $\langle G(q|k)\rangle$ is required to be diagonal in q and k,

$$\langle G(q|k)\rangle = 2\pi\delta(q-k)G(q,\omega) , \quad \text{(A15)}$$

where

$$G(q,\omega)=\frac{1}{G_0^{-1}(q,\omega)-M(q,\omega)} . \quad \text{(A16)}$$

The proper self-energy $M(q,\omega)$ appearing in Eq. (A16) is given by

$$M(q,\omega)=\delta^2\left[(\epsilon_d-1)\frac{\omega^2}{c^2}\right]^2\int_{-\infty}^{\infty}\frac{dp}{2\pi}g(|q-p|)G_0(p,\omega) \quad \text{(A17)}$$

in the small roughness approximation.

To calculate the two-particle Green's function $\langle |G(q|k)|^2\rangle$ needed in the evaluation of Eq. (A9) we consider the more general two-particle Green's function $\langle G(p+|p'+)G^*(p-|p'-)\rangle$, where $p\pm=p\pm q/2$ and $p'\pm=p'\pm q/2$, and take the limit as $q\to 0$ at the end of the calculation. Due to the stationarity of $\zeta(x_1)$, this function can be written in the form

$$\langle G(p+|p'+)G^*(p-|p'-)\rangle = L_1\phi_{pp'}(q) , \quad \text{(A18)}$$

where the reduced two-particle Green's function $\phi_{pp'}(q)$ satisfies the Bethe-Salpeter equation[15]

$$\phi_{pp'}(q)=2\pi\delta(p-p')G(p+,\omega)G^*(p-,\omega)$$
$$+G(p+,\omega)G^*(p-,\omega)$$
$$\times\int_{-\infty}^{\infty}\frac{ds}{2\pi}U_{ps}(q)\phi_{sp'}(q)\ , \tag{A19}$$

where $U_{ps}(q)$ is the irreducible vertex function.

The solution of Eq. (A19) can be written formally as

$$\phi_{pp'}(q)=2\pi\delta(p-p')G(p+,\omega)G^*(p-,\omega)$$
$$+G(p+,\omega)G^*(p-,\omega)R_{pp'}(q)$$
$$\times G(p'+,\omega)G^*(p'-,\omega)\ , \tag{A20}$$

where $R_{pp'}(q)$ is the reducible vertex function, and is the solution of the equation

$$R_{pp'}(q)=U_{pp'}(q)$$
$$+\int_{-\infty}^{\infty}\frac{ds}{2\pi}U_{ps}(q)G(s+,\omega)G^*(s-,\omega)R_{sp}(q)\ . \tag{A21}$$

If we now note that, since

$$|\langle G(p|p')\rangle|^2=[2\pi\delta(p-p')]^2|G(p,\omega)|^2$$
$$=L_1 2\pi\delta(p-p')|G(p,\omega)|^2\ , \tag{A22}$$

then on combining the results given by Eqs. (A18) and (A20) with the expression for $\langle\partial R_s/\partial\theta_s\rangle_{\rm incoh}$ given by Eq. (A9), we obtain the result that

$$\left\langle\frac{\partial R_s}{\partial\theta_s}\right\rangle_{\rm incoh}=\frac{2}{\pi}\left[\frac{\omega}{c}\right]^3\cos^2\theta_s\cos\theta_0$$
$$\times|G(q,\omega)|^2R_{qk}(0)|G(k,\omega)|^2\ , \tag{A23}$$

where we recall that $q=(\omega/c)\sin\theta_s$ and $k=(\omega/c)\sin\theta_0$.

To solve Eq. (A21) we need an approximation to the irreducible vertex function $U_{pp'}(q)$ that enters it. We will approximate it by the expression that corresponds to the sum of all maximally crossed diagrams in diagrammatic perturbation theory. It is this contribution that describes the coherent interference between each multiple-scattering sequence and its time-reversed partner that is responsible for the effects being studied in this paper.[16] To obtain this expression we first assume for $U_{pp'}(q)$ the lowest-order approximation to it in $\zeta(x_1)$, $U^{(0)}_{pp'}(q)$, which is obtained from the result that[15]

$$\langle V^{(1)}(p+|p-)V^{(1)}(p'+|p''-)^*\rangle$$
$$=2\pi\delta(p'-p'')U^{(0)}_{pp'}(q)$$
$$=2\pi\delta(p'-p'')\left[(\epsilon_d-1)\frac{\omega^2}{c^2}\right]^2\delta^2 g(|p-p'|)\ . \tag{A24}$$

Thus, we find that $U^{(0)}_{pp'}(q)$ is in fact independent of q and can be written in the form

$$U^{(0)}_{pp'}=W^2 g(|p-p'|)\ , \tag{A25}$$

where

$$W=\delta(\epsilon_d-1)\frac{\omega^2}{c^2}\ . \tag{A26}$$

In the language of diagrammatic perturbation theory, the vertex function $U^{(0)}_{pp'}$ corresponds to a single rung of a ladder diagram.

When the surface height correlation function $W(|x_1|)=\exp(-x_1^2/a^2)$ is a sharp function, i.e., when the transverse correlation length a is small, we can solve Eq. (A21) analytically. This is because in a convolution integral containing the power spectrum of the surface roughness,

$$\int_{-\infty}^{\infty}\frac{ds}{2\pi}g(|p-s|)f(s)\ ,$$

we can make the replacement $g(|p-s|)\rightarrow g(|p|)g(|s|)/g(0)$ in this limit.[17] As a consequence, Eq. (A21) becomes an integral equation with a separable kernel,

$$R^{(L)}_{pp'}(q)=U^{(0)}_{pp'}+W^2\frac{g(|p|)}{g(0)}$$
$$\times\int_{-\infty}^{\infty}\frac{ds}{2\pi}g(|s|)K_s(q)R^{(L)}_{sp'}(q)\ , \tag{A27}$$

where the superscript L denotes that the solution of this equation is the contribution to the reducible vertex function from the ladder diagrams, and where we have simplified the notation by defining

$$K_s(q)\equiv G(s+,\omega)G^*(s-,\omega) \tag{A28a}$$
$$=K^*_{-s}(q)\ . \tag{A28b}$$

The solution of Eq. (A27) is

$$R^{(L)}_{pp'}(q)=U^{(0)}_{pp'}+W^4\frac{g(|p|)}{g(0)}\frac{I(q)}{1-\frac{W^2}{g(0)}I(q)}\frac{g(|p'|)}{g(0)}\ , \tag{A29}$$

where

$$I(q)=\int_{-\infty}^{\infty}\frac{ds}{2\pi}g^2(|s|)K_s(q) \tag{A30a}$$

$$=\frac{1}{\pi}\int_0^{\infty}ds\,g^2(s)\mathrm{Re}K_s(q)\ . \tag{A30b}$$

In obtaining Eq. (A30b) we have used Eq. (A28b).

We next carry out the transformations $p\rightarrow\frac{1}{2}q+\frac{1}{2}(p-p')$, $p'\rightarrow\frac{1}{2}q-\frac{1}{2}(p-p')$, and $q\rightarrow p+p'$ in the result given by Eq. (A29). They transform $R_{pp'}^{(L)}(q)$ into $U_{pp'}^{(\mathrm{MC})}(q)$, the contribution to the irreducible vertex from the maximally-crossed diagrams in diagrammatic perturbation theory.[18] The result is

$$U_{pp'}^{(\mathrm{MC})}(q)=U_{pp'}^{(0)}+W^4\frac{g(\frac{1}{2}|p-p'|)}{g(0)}\frac{I(p+p')}{1-\dfrac{W^2}{g(0)}I(p+p')}\times\frac{g(\frac{1}{2}|p-p'|)}{g(0)}$$

$$\equiv U_{pp'}^{(0)}+\Lambda_{pp'}\ , \tag{A31}$$

where we have used the result that $U_{pp'}^{(0)}$ is invariant under these transformations, and have passed to the limit $q\rightarrow 0$ in terms where this produces no singularities. Equation (A31) is the approximation to the irreducible vertex function we will use in solving Eq. (A21).

To proceed beyond this point we must analyze the form of the vertex function $\Lambda_{pp'}$ in its dependence on p and p', and for this we need the structure of the function $K_s(q)$ defined by Eq. (A28).

The Green's function $G(q,\omega)$ Eq. (A16), has poles at the wave numbers of the guided waves supported by the scattering structure corresponding to the frequency ω of the incident light. We will exploit this circumstance to simplify the subsequent calculations by making a pole approximation to $G(q,\omega)$ for a two-mode system of the form

$$G(q,\omega)=\sum_m\frac{C_m(\omega)}{q-q_m(\omega)-i\Delta_m(\omega)}\ . \tag{A32}$$

In this expression the summation index m takes the values -2, -1, 1, 2, and $C_{-m}(\omega)=-C_m(\omega)$, $q_{-m}(\omega)=-q_m(\omega)$, and $\Delta_{-m}(\omega)=-\Delta_m(\omega)$. Here $q_1(\omega)$ and $q_2(\omega)$ are the wave numbers of the two guided waves, while $\Delta_1(\omega)$ and $\Delta_2(\omega)$ are their decay rates. In writing Eq. (A32), we have neglected the shifts in the values of $q_1(\omega)$ and $q_2(\omega)$, obtained in Sec. III in the absence of surface roughness, that arise from the real part of the self-energy $M(q,\omega)$, and have used for $C_1(\omega)$ and $C_2(\omega)$ the residues at the poles $q=q_1(\omega)$ and $q=q_2(\omega)$ of the unperturbed Green's function, $G_0(q,\omega)$. The decay rate $\Delta_m(\omega)$ $(m=1,2)$ has been written as the sum $\Delta_m^{(\epsilon)}(\omega)+\Delta_m^{\mathrm{gw}}(\omega)$, where $\Delta_m^{(\epsilon)}(\omega)$ is the decay rate of the guided wave m associated with the imaginary part of the dielectric constant of the film, while $\Delta_m^{(\mathrm{gw})}(\omega)$ is the decay rate due to the roughness induced conversion of the guided wave into other guided waves and into volume electromagnetic waves. The former was obtained numerically from a study of $G_0^{-1}(q,\omega)$ in the vicinity of $q=q_m(\omega)$. The latter is given by $\Delta_m^{(\mathrm{gw})}(\omega)=C_m(\omega)\mathrm{Im}M[q_m(\omega),\omega]$. For a dielectric film of mean thickness $d=500$ nm and dielectric constant $\epsilon_d=2.6896+i0.0075$, illuminated by s-polarized light of wavelength $\lambda=632.8$ nm, we find that $q_1(\omega)=1.5466(\omega/c)$, $q_2(\omega)=1.2423(\omega/c)$, $C_1(\omega)=0.019\,56$, $C_2=0.086\,39$, while $\Delta_1^{(\epsilon)}(\omega)=0.002\,34(\omega/c)$, $\Delta_1^{(\mathrm{gw})}(\omega)=0.000\,54(\omega/c)$, $\Delta_2^{(\epsilon)}(\omega)=0.002\,56(\omega/c)$, and $\Delta_2^{(\mathrm{gw})}(\omega)=0.002\,73(\omega/c)$. In obtaining the values of $\Delta_1^{(\mathrm{gw})}(\omega)$ and $\Delta_2^{(\mathrm{gw})}(\omega)$ we have assumed that the roughness of the vacuum-dielectric interface is characterized by the parameters $\delta=15$ nm and $a=100$ nm.

The substitution of Eq. (A32) into Eq. (A28a), together with a partial fraction decomposition of the product of the Green's functions, yields the result

$$K_s(q)\cong\sum_m\sum_n\frac{C_mC_n}{i(\Delta_m+\Delta_n)+(q_m-q_n)-q}\times\left[\frac{1}{s-q_m-i\Delta_m}-\frac{1}{s-q_n+i\Delta_n}\right]\ , \tag{A33}$$

in the limit $q\rightarrow 0$. In the double sum we retain only the terms that are large for small values of q. This reduces the expressions (A33) to

$$K_s(q)\cong\sum_m\frac{C_m^2}{2i\Delta_m-q}\frac{2i\Delta_m}{(s-q_m)^2+\Delta_m^2}+C_1C_2\left\{\frac{1}{i(\Delta_1+\Delta_2)+(q_2-q_1-q)}\left[\frac{1}{s-q_2-i\Delta_2}-\frac{1}{s-q_1+i\Delta_1}\right]\right.$$

$$+\frac{1}{-i(\Delta_1+\Delta_2)+(q_2-q_1-q)}\left[\frac{1}{s+q_1+i\Delta_1}-\frac{1}{s+q_2-i\Delta_2}\right]$$

$$+\frac{1}{i(\Delta_1+\Delta_2)+(q_2-q_1+q)}\left[\frac{1}{s-q_1-i\Delta_1}-\frac{1}{s-q_2+i\Delta_2}\right]$$

$$\left.+\frac{1}{-i(\Delta_1+\Delta_2)+(q_2-q_1-q)}\left[\frac{1}{s+q_2+i\Delta_2}-\frac{1}{s+q_1-i\Delta_1}\right]\right\}\ . \tag{A34}$$

It is only the real part of $K_s(q)$ that is needed for evaluating the function $I(q)$ defined by Eq. (A30b), and from Eq. (A34) we find that this is given by

$$\begin{aligned}\mathrm{Re}K_s(q)=&\sum_m C_m^2\frac{4\Delta_m}{4\Delta_m^2+q^2}\frac{\Delta_m}{(s-q_m)^2+\Delta_m^2}\\&+C_1C_2\left\{\frac{1}{(\Delta_1+\Delta_2)^2+(q_2-q_1-q)^2}\right.\\&\times\left[\frac{\Delta_1(\Delta_1+\Delta_2)-(q_2-q_1-q)(s-q_1)}{(s-q_1)^2+\Delta_1^2}+\frac{\Delta_1(\Delta_1+\Delta_2)+(q_2-q_1-q)(s+q_1)}{(s+q_1)^2+\Delta_1^2}\right.\\&\left.+\frac{\Delta_2(\Delta_1+\Delta_2)+(q_2-q_1-q)(s-q_2)}{(s-q_2)^2+\Delta_2^2}+\frac{\Delta_2(\Delta_1+\Delta_2)-(q_2-q_1-q)(s+q_2)}{(s+q_2)^2+\Delta_2^2}\right]\\&+\frac{1}{(\Delta_1+\Delta_2)^2+(q_2-q_1+q)^2}\\&\times\left[\frac{\Delta_1(\Delta_1+\Delta_2)-(q_2-q_1+q)(s-q_1)}{(s-q_1)^2+\Delta_1^2}+\frac{\Delta_1(\Delta_1+\Delta_2)+(q_2-q_1+q)(s+q_1)}{(s+q_1)^2+\Delta_1^2}\right.\\&\left.\left.+\frac{\Delta_2(\Delta_1+\Delta_2)+(q_2-q_1+q)(s-q_2)}{(s-q_2)^2+\Delta_2^2}+\frac{\Delta_2(\Delta_1+\Delta_2)-(q_2-q_1+q)(s+q_2)}{(s+q_2)^2+\Delta_2^2}\right]\right\}.\end{aligned}\tag{A35}$$

We again drop all terms that are small when q is small, and obtain

$$\begin{aligned}\mathrm{Re}K_s(q)=&C_1^2\frac{4\Delta_1}{4\Delta_1^2+q^2}\frac{\Delta_1}{(s-q_1)^2+\Delta_1^2}+C_2^2\frac{4\Delta_2}{4\Delta_2^2+q^2}\frac{\Delta_2}{(s-q_2)^2+\Delta_2^2}\\&+C_1C_2\left[\frac{\Delta_1+\Delta_2}{(\Delta_1+\Delta_2)^2+(q_2-q_1-q)^2}+\frac{\Delta_1+\Delta_2}{(\Delta_1+\Delta_2)^2+(q_2-q_1+q)^2}\right]\\&\times\left[\frac{\Delta_1}{(s-q_1)^2+\Delta_1^2}+\frac{\Delta_2}{(s-q_2)^2+\Delta_2^2}\right].\end{aligned}\tag{A36}$$

In writing Eq. (A36) we have also dropped all functions of s that are not resonant at a positive value of s, since the integration in Eq. (A30b) extends only over such values of s. With the approximation

$$\frac{\Delta}{(s-q)^2+\Delta^2}\cong\pi\delta(s-q)\,,\tag{A37}$$

by combining Eqs. (A30b) and (A36) we obtain finally,

$$\begin{aligned}I(q)=&4\pi a^2\left[\frac{C_1^2\Delta_1}{4\Delta_1^2+q^2}e^{-(a^2/2)q_1^2}+\frac{C_2^2\Delta_2}{4\Delta_2^2+q^2}e^{-(a^2/2)q_2^2}\right]\\&+\pi a^2C_1C_2\left[\frac{\Delta_1+\Delta_2}{(\Delta_1+\Delta_2)^2+(q_2-q_1-q)^2}+\frac{\Delta_1+\Delta_2}{(\Delta_1+\Delta_2)^2+(q_2-q_1+q)^2}\right](e^{-(a^2/2)q_1^2}+e^{-(a^2/2)q_2^2}),\end{aligned}\tag{A38}$$

where we have used the Gaussian form (2.8) for the power spectrum of the surface roughness. It follows from Eq. (A38) that

$$\begin{aligned}I(p+p')=&4\pi a^2\left[\frac{C_1^2\Delta_1}{4\Delta_1^2+(p+p')^2}e^{-(a^2/2)q_1^2}+\frac{C_2^2\Delta_2}{4\Delta_2^2+(p+p')^2}e^{-(a^2/2)q_2^2}\right]\\&+\pi a^2C_1C_2\left[\frac{\Delta_1+\Delta_2}{(\Delta_1+\Delta_2)^2+(q_2-q_1-p-p')^2}+\frac{\Delta_1+\Delta_2}{(\Delta_1+\Delta_2)^2+(q_2-q_1+p+p')^2}\right](e^{-(a^2/2)q_1^2}+e^{-(a^2/2)q_2^2}).\end{aligned}\tag{A39}$$

When the result given by Eq. (A39) is substituted into Eq. (A31), we find that the vertex function $\Lambda_{pp'}$ is large when $p+p'\approx 0$ due to the first two terms on the right-hand side of Eq. (A39)—this gives rise to the enhanced backscattering peak in $\langle\partial R_s/\partial\theta_s\rangle_{\mathrm{incoh}}$—and it is also large when $p+p'\cong\pm(q_2-q_1)$, due to the third and fourth terms on the right-hand side of this equation—this gives rise to two satellite peaks, one on each side of the enhanced backscattering peak.

The Neumann-Liouville solution of Eq. (A21) in the

limit $q \to 0$ has the form

$$R_{pp'}(0) = U_{pp'}^{(\mathrm{MC})} + \int_{-\infty}^{\infty} \frac{ds}{2\pi} U_{ps}^{(\mathrm{MC})} |G(s,\omega)|^2 U_{sp'}^{(\mathrm{MC})} + \cdots$$
$$= [U_{pp'}^{(0)} + \Lambda_{pp'}] + \int_{-\infty}^{\infty} \frac{ds}{2\pi} [U_{ps}^{(0)} + \Lambda_{ps}] |G(s,\omega)|^2 \times [U_{sp'}^{(0)} + \Lambda_{sp'}] \cdots . \quad \text{(A40)}$$

In summing this series we keep the complete first term, but keep only the terms containing $U_{pp'}^{(0)}$ alone in the remaining integral terms. The reason for this is that $|G(s,\omega)|^2$ is large only for $s \cong \pm q_{1,2}(\omega)$, i.e., for wave numbers s outside the radiative region $(-\omega/c, \omega/c)$. On the other hand $\Lambda_{pp'}$ is large only when $p+p'=0, \pm[q_2(\omega)-q_1(\omega)]$. Both p and p' are required to be inside the radiative region in the calculation of $\langle \partial R_s/\partial\theta_s \rangle_{\mathrm{incoh}}$. Thus, the terms containing $\Lambda_{pp'}$ in all integral terms on the right-hand side of Eq. (A40) give only a small correction to the first term, either because they are off-resonance, $p+p' \neq 0, \pm[q_2(\omega)-q_1(\omega)]$, or else are multipled by higher powers of the small ratio δ^2/a^2 than the first, when they are resonant. The contribution from the terms in the infinite series on the right-hand side of Eq. (A40) that contain only $U_{pp'}^{(0)}$ is just $R_{pp'}^{(L)}(0)$, where $R_{pp'}^{(L)}(q)$ is given by Eq. (A29). Our final result for $R_{pp'}(0)$ is, therefore,

$$R_{pp'}(0) = U_{pp'}^{(0)} + W^4 \frac{g(|p|)}{g(0)} \frac{I(0)}{1 - \frac{W^2}{g(0)} I(0)} \frac{g(|p'|)}{g(0)} + W^4 \frac{g(\frac{1}{2}|p-p'|)}{g(0)} \frac{I(p+p')}{1 - \frac{W^2}{g(0)} I(p+p')} \times \frac{g(\frac{1}{2}|p-p'|)}{g(0)} . \quad \text{(A41)}$$

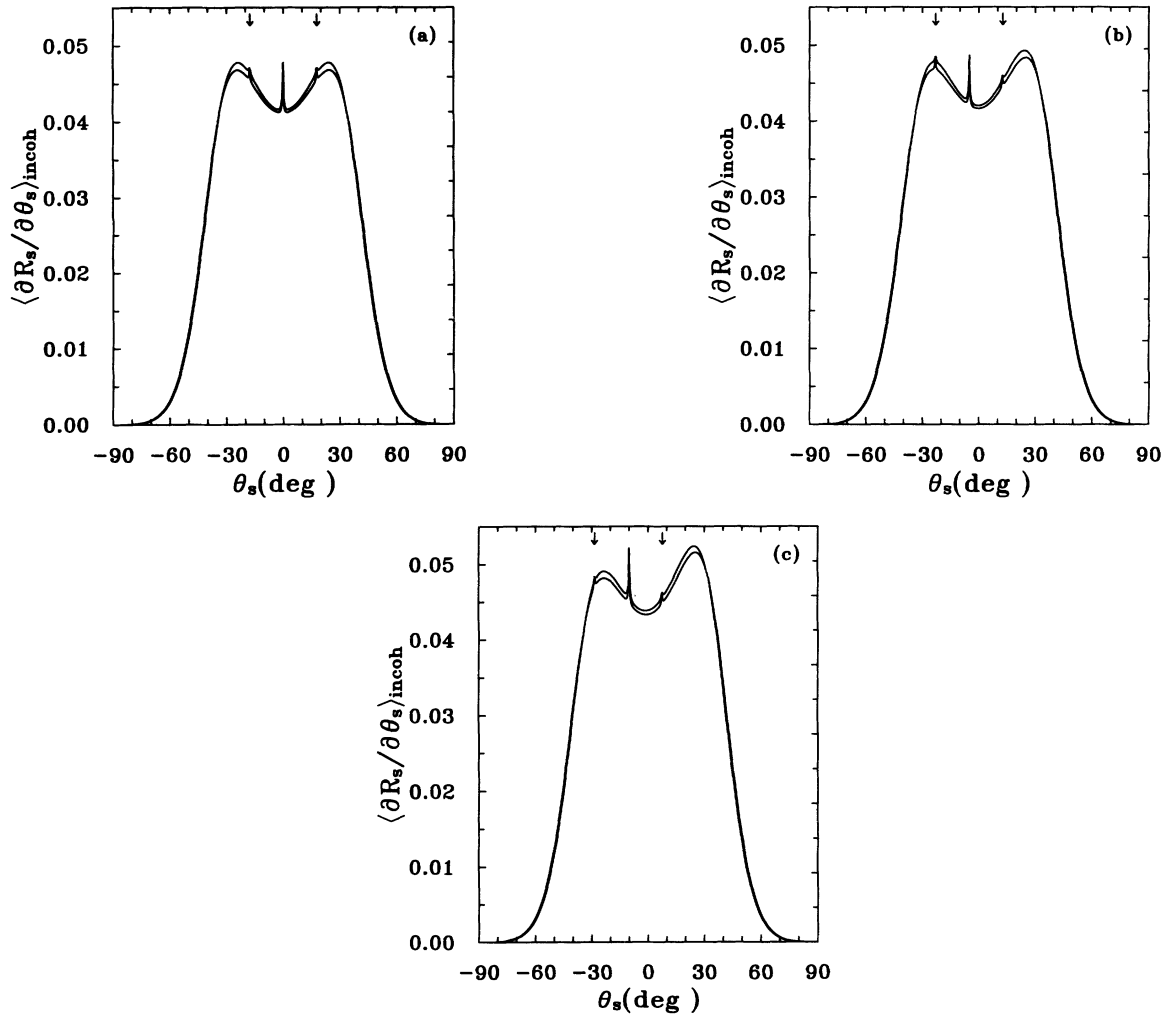

FIG. 9. A plot of $\langle \partial R_s/\partial\theta_s \rangle_{\mathrm{incoh}}$ as a function of the scattering angle for the scattering of s-polarized light of wavelength $\lambda = 632.8$ nm, incident on a dielectric film of mean thickness $d = 500$ nm, and dielectric constant $\epsilon_d = 2.6896 + i0.0075$, deposited on a planar perfectly conducting substrate. The one-dimensional, randomly rough, vacuum-dielectric interface is characterized by the parameter $\delta = 15$ nm and $a = 100$ nm. The results obtained by the many-body perturbation calculation carried out in the Appendix (upper curve) and by the small-amplitude perturbation theory carried out in Sec. IV (lower curve) are presented. (a) $\theta_0 = 0°$, (b) $\theta_0 = 5°$, (c) $\theta_0 = 10°$.

In Fig. 9 we plot the contribution to the mean differential reflection coefficient from the incoherent component of the scattered light, $\langle \partial R_s/\partial\theta_s \rangle_{\text{incoh}}$, as a function of the scattering angle θ_s, that is obtained when the result given by Eqs. (A25), (A26), (A38), (A39), and (A41) are used in Eq. (A23). The Gaussian form of the power spectrum of the surface roughness, Eq. (2.8), has been used in these calculations, and the experimental and roughness parameters assumed are those used in obtaining the values of $q_{1,2}(\omega)$, $\Delta_{1,2}(\omega)$, and $C_{1,2}(\omega)$ quoted following Eq. (A32) above. The enhanced backscattering peak and its two satellite peaks are clearly visible in the results plotted in Fig. 9. The positions of the satellite peaks are at scattering angles given by $\sin\theta_s = -\sin\theta_0 \pm (c/\omega)[q_2(\omega) - q_1(\omega)]$. For comparison, we have also plotted the results for $\langle \partial R_s/\partial\theta_s \rangle_{\text{incoh}}$ obtained from the third-order perturbation calculation carried out in Sec. IV for the same values of the experimental and roughness parameters. It is seen that although there are some small quantitative differences between the two sets of results, they are in quite good overall agreement with each other. This suggests that the approximations made in this Appendix in order to obtain an analytic result are valid for the experimental and roughness parameters assumed in the calculation leading to Fig. 9.

[1] I. M. Lifshitz, S. A. Gredeskul, and L. A. Pastur, *Introduction to the Theory of Disordered Systems* (Wiley, New York, 1988).

[2] V. D. Freililkher and S. A. Gredeskul, J. Opt. Soc. Am. A 7, 868 (1990).

[3] E. Abrahams, P. W. Anderson, D. C. Licciardello, and T. V. Ramakrishnan, Phys. Rev. Lett. **42**, 673 (1979).

[4] A. R. McGurn, A. A. Maradudin, and V. Celli, Phys. Rev. B **31**, 4866 (1985).

[5] I. Freund, M. Rosenbluh, and R. Berkovits, Phys. Rev. B **39**, 12 403 (1989).

[6] V. D. Freilikher, M. Pustilnik, and I. Yurkevich, Phys. Lett. A (to be published).

[7] A. A. Maradudin and E. R. Méndez, Appl. Opt. **32**, 3335 (1993).

[8] Lord Rayleigh, *The Theory of Sound,* 2nd ed. (MacMillan, London, 1896), Vol. II, pp. 89 and 96.

[9] Lord Rayleigh, Proc. R. Soc. London Ser. A **79**, 399 (1907).

[10] J. A. Ogilvy, *Theory of Wave Scattering from Random Rough Surfaces* (Hilger, London, 1991).

[11] Jun Q. Lu, A. A. Maradudin, and T. Michel, J. Opt. Soc. Am. B **8**, 311 (1991).

[12] A. A. Maradudin, T. Michel, A. R. McGurn, and E. R. Méndez, Ann. Phys. (N.Y.) **203**, 255 (1990).

[13] A. A. Maradudin, E. R. Méndez, and T. Michel, in *Scattering in Volumes and Surfaces,* edited by M. Nieto-Vesperinas and J. C. Dainty (North-Holland, Amsterdam, 1990), p. 157.

[14] G. C. Brown, V. Celli, M. Coopersmith, and M. Haller, Surf. Sci. **129**, 507 (1983).

[15] A. R. McGurn, A. A. Maradudin, and V. Celli, Phys. Rev. B **31**, 4866 (1985).

[16] G. Bergmann, Phys. Rev. B **28**, 2914 (1983); D. E. Khmel'nitskii, Physica B **126**, 235 (1984).

[17] T. N. Antsygina, V. D. Freylikher, S. A. Gredeskul, L. A. Pastur, and V. A. Slusarev, J. Electromagn. Waves Appl. **5**, 873 (1991).

[18] D. Vollhardt and P. Wölfle, Phys. Rev. B **22**, 4666 (1980).

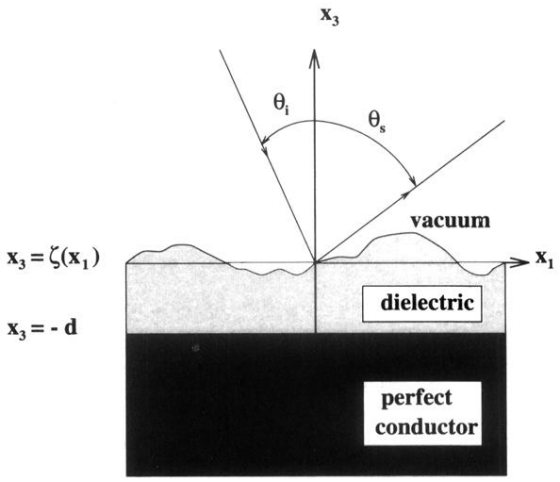

FIG. 2. The scattering system studied in this work.